Optica Applicata, Vol. XVIII, No. 1, 1988

Variable wavelength interferometry VII. Object-adapted method

MAKSYMILIAN PLUTA

Central Optical Laboratory, ul. Kamionkowska 18, 03–805 Warszawa, Poland.

The variable wavelength interferometric techniques described previously incorporate an idea of two specific procedures referred to as adaptive variable wavelength interferometry (AVAWI). One of these procedures functions in the wavelength domain and the other, in the domain of interfringe spacings. The latter appears to be more useful for transmitted light interferometry than the former. On the other hand, the former is more suitable for reflected-light interferometry of objects surrounded by an air medium.

1. Introduction

Three versions of variable wavelength interferometry (VAWI) were described in previous papers. Their specific feature is the fact that the interfringe spacing (b) is the only parameter measured directly, while other quantities are observed, read out from the calibration plot $b(\lambda)$, and derived from quite simple formulae.

The VAWI–1 technique [1]–[3] depends on selecting such particular wavelengths $\lambda_s = \lambda_1 > \lambda_2 > \lambda_3, \ldots$, for which interference fringes displaced by an object under study become consecutively coincident and anticoincident side by side with the reference (undisplaced) fringes; thus, interference order increments $q_s = 0, 0.5, 1, \ldots$ are observed. This technique is suitable for studying the objects which produce optical path differences (δ) greater than several wavelengths, say, $\delta > 3\lambda_1$.

On the other hand, the VAWI–2 technique is suitable for determining $\delta < 3\lambda_1$. This technique uses two parallel pointer lines in the image plane of the interferometer [4], [5]. The zero-order fringe of the empty interference field is adjusted to the coincidence with one pointer line, and high-order fringes of this field and next those displaced by the object under study are consecutively brought into coincidence with the other pointer line when the wavelength of monochromatic light is varied.

The VAWI–3 technique is similar to VAWI–1 technique, but it uses a single pointer line and does not require simultaneous observation of the reference and displaced interference fringes.

All these techniques incorporate an idea of a specific method, which can be called adaptive variable wavelength interferometry (AVAWI).

2. Principle of the AVAWI method

Conventional interferometric techniques permit us generally to determine optical path diffrences δ from a quite simple relation

$$\delta = \frac{c}{b}\lambda \tag{1}$$

where b is the interfringe spacing, c is the fringe displacement produced by an object under study, and λ is the wavelength of light used. Equation (1) can formally be rewritten as

$$\delta = (m_1 + q)\lambda = m\lambda \tag{2}$$

where m_1 is a suitably selected integer number, m is referred to as the current interference order ($m = c/b$), and q is the increment (or decrement) of this order with respect to m_1. From Eqs. (1) and (2) it follows that

$$(m_1 + q)b = c. \tag{3}$$

The above relations are quite trivial, but they will be useful for the further discussion.

Without restricting in any way the generality of the results, we assume that a fringe interference field is produced by superposition of two plane wavefronts inclined to each other at a small angle ε. The empty interference field, i.e., the interference pattern not perturbed by the object under study, is covered by equally spaced straight-line fringes. The dark fringes occur for the optical path differences $\Delta = 0, \pm\lambda, \pm 2\lambda, \ldots$ and bright ones for $\Delta = \pm\lambda/2, \pm 3\lambda/2, \pm 5\lambda/2, \ldots$. This is, for instance, the case of the polarization interference system whose polarizer and analyser are crossed. Such an interferometer will especially be taken into consideration.

In all VAWI techniques presented previously [1]–[6], the formula

$$m_1 = q_s \frac{\lambda_s}{\lambda_1 - \lambda_s} \tag{4}$$

was used for calculating the initial interference order m_1 corresponding to the wavelength λ_1, from which the current interference order $m_s = m_1 + q_s$ was increased by continuous decreasing the light wavelength λ from λ_1 to $\lambda_s = \lambda_2, \lambda_3, \lambda_4, \ldots$. Usually, the interference order increments q_s were selected to be equal to 1, 2, 3, ... or 0.5, 1, 1.5, 2, ..., respectively for $\lambda_s = \lambda_2 > \lambda_3 > \lambda_4 \ldots$.

In general, Eq. (4) was used as only an approximative formula. However, there are interferometric situations where Eq. (4) is ideally true. These situations are qualified as object-adapted or adaptive variable wavelength interferometry in the wavelength domain. Interferometry of this kind will shortly be denoted by AVAWI(λ).

As can readily be seen, Eq. (4) may be rewritten as

$$(m_1 + q_s)\lambda_s = m_1 \lambda_1. \tag{5}$$

Table 1. Conditions for transmitted-light AVAWI using different VAWI techniques

Symbol the VAWI technique and references	Initial interference order m_1 expressed by		Conditions for	
	light wavelengths (λ)	interfringe spacings (b)	AVAWI(λ)	AVAWI(b)
VAWI–1, [1], [2]	$m_1 = q_s \frac{\lambda_s}{N'_{s1}\lambda_1 - \lambda_s}$ where $N'_{s1} = (n'_s - n_s)/(n'_1 - n_1)$	$m_1 = q_s \frac{b_s}{N'_{s1}\varepsilon_{1s} b_1 - b_s}$ where $\varepsilon_{1s} = \varepsilon_1/\varepsilon_s$	$N'_{s1} = 1$	$N'_{s1}\varepsilon_{1s} = 1$
VAWI–2, [4], [5], [6]	for the empty interference field		for the empty interference field	
	$m_1 = q_s \frac{\lambda_s}{\varepsilon_{s1}\lambda_1 - \lambda_s}$ where $\varepsilon_{s1} = \varepsilon_s/\varepsilon_1$	$m_1 = q_s \frac{b_s}{b_1 - b_s}$	$\varepsilon_{s1} = 1$	no condition (–)
	for the image of an object under study		for the object image	
	$m_1 = q_s \frac{\lambda_s}{N'_{s1}\lambda_1 - \lambda_s} + d\frac{N'_{s1}\varepsilon_1 - \varepsilon_s}{N'_{s1}\lambda_1 - \lambda_s}$	$m_1 = q_s \frac{b_s}{N'_{s1}\varepsilon_{1s} b_1 - b_s} + d\frac{N'_{s1}\varepsilon_{1s} - 1}{N'_{s1}\varepsilon_{1s} b_1 - b_s}$	$N'_{s1} = 1$ and $\varepsilon_s = \varepsilon_1$	$N'_{s1}\varepsilon_{1s} = 1$
VAWI–3, [5]	for the empty interference field		for the empty interence field	
	$m_1 = 0$	$m_1 = 0$	(–)	(–)
	for the image of an object under study		for the object image	
	$m_1 = q_s \frac{\lambda_s}{N'_{s1}\lambda_1 - \lambda_s}$	$m_1 = q_s \frac{b_s}{N'_{s1}\varepsilon_{1s} b_1 - b_s}$	$N'_{s1} = 1$	$N'_{s1}\varepsilon_{1s} = 1$

Explanations: n – refractive index of the object under study, n' – refractive index of a medium which surrounds the object, q_s – increments of the current interference orders $m_s = m_1 + q_s$, which corresponds to the light wavelengths λ_s.

Notes: 1. The increments q_s were denoted by q_2 in [1]–[4], and the wavelengths λ_s by λ_2; 2. The interfringe spacings b_s were denoted by b_2 in [2], [4]; 3. The coefficients N'_{s1} were denoted by N_{21} in [1], [2], [4]; 4. The coefficients ε_{1s} were denoted by k_{12} in [2]; 5. If the birefringence (B) of double-refracting objects is directly measured, the coefficient N'_{s1} in the equations and conditions listed above is replaced by the coefficient $B_{s1} = B_s/B_1$; 6. When a double-refracting interferometer, like Biolar PI microinterferometer, is used, the coefficients $\varepsilon_{1s} = D_{1s} = D_1/D_s$ and $\varepsilon_{1s} = D_{1s} = D_1/D_s$, where D is the birefringence of the material of which the main Wollaston prism of the interferometer is made.

Table 2. Conditions for the reflected-light AVAWI using different VAWI techniques

Symbol of the VAWI technique and Refs.	Initial interference order m_1 expressed by		Conditions for	
	light wavelengths (λ)	interfringe spacings (b)	AVAWI(λ)	AVAWI(b)
VAWI–1, [3]	$m_1 = q_s \frac{\lambda_s}{n'_{s1}\lambda_1 - \lambda_s} + \frac{n'_{s1}\lambda_1\psi_1 - \lambda_s\psi_s}{2\pi(n'_{s1}\lambda_1 - \lambda_s)}$	$m_1 = q_s \frac{b_s}{n'_{s1}\varepsilon_{1s}b_1 - b_s} + \frac{n'_{s1}\varepsilon_{1s}b_1\psi_1 - b_s\psi_s}{2\pi(n'_{s1}\varepsilon_{1s}b_1 - b_s)}$	$n'_{s1} = 1$	$n'_{s1}\varepsilon_{1s} = 1$
	where $n'_{s1} = n'_s/n'_1$		and $\lambda_s\psi_s = \lambda_1\psi_1$	and $b_s\psi_s = b_1\psi_1$
	If the phase jump differences $\psi_s = \psi_1 = \psi$		If $\psi_s = \psi_1 = \psi$	
	$m_1 = q_s \frac{\lambda_s}{n'_{s1}\lambda_1 - \lambda_s} + \frac{\psi}{2\pi}$	$m_1 = q_s \frac{b_s}{n'_{s1}\varepsilon_{1s}b_1 - b_s} + \frac{\psi}{2\pi}$	$n'_{s1} = 1$	$n'_{s1}\varepsilon_{1s} = 1$
			and $\psi = 0$	and $\psi = 0$
	If the phase jump differences $\psi_s = \psi_1 = \psi = 0$ and $n'_{s1} = 1$		If $\psi_s = \psi_1 = \psi = 0$	
	$m_1 = q_s \frac{\lambda_s}{\lambda_1 - \lambda_s}$	$m_1 = q_s \frac{b_s}{\varepsilon_{1s}b_1 - b_s}$		and $n'_{s1} = 1$
			(–)	$\varepsilon_{1s} = 1$
	for the empty interference field (EIF)		for EIF	
VAWI–2, [4]	$m_1 = q_s \frac{\lambda_s}{\varepsilon_{s1}\lambda_1 - \lambda_s}$	$m_1 = q_s \frac{b_s}{b_1 - b_s}$	$\varepsilon_{s1} = 1$	(–)
	for the object image (OI) if $\psi_s = \psi_1 = \psi = 0$		for OI if $\psi = 0$	
	$m_1 = q_s \frac{\lambda_s}{n'_{s1}\lambda_1 - \lambda_s} + d\frac{n'_{s1}\varepsilon_1 - \varepsilon_s}{n'_{s1}\lambda_1 - \lambda_s}$	$m_1 = q_s \frac{b_s}{n'_{s1}\varepsilon_{1s}b_1 - b_s} + d\frac{n'_{s1}\varepsilon_{1s} - 1}{n'_{s1}\varepsilon_{1s}b_1 - b_s}$	$n'_{s1} = 1$	$n'_{s1}\varepsilon_{1s} = 1$
			and $\varepsilon_s = \varepsilon_1$	
	for the object image if $\psi_1 = \psi_2 = \psi = 0$ and $n'_{s1} = 1$ (air medium)		for OI if $\psi = 0$ and $n'_{s1} = 1$	
	$m_1 = q_s \frac{\lambda_s}{\lambda_1 - \lambda_s} + d\frac{\varepsilon_1 - \varepsilon_s}{\lambda_1 - \lambda_s}$	$m_1 = q_s \frac{b_s}{\varepsilon_{1s}b_1 - b_s} + d\frac{\varepsilon_{1s} - 1}{\varepsilon_{1s}b_1 - b_s}$	$\varepsilon_s = \varepsilon_1$	$\varepsilon_{1s} = 1$ or $\varepsilon_s = \varepsilon_1$

	for the empty interference field		for EIF	
VAWI–3	$m_1 = 0$	$m_1 = 0$	(−)	(−)
	for the object image if $\psi_s = \psi_1 = \psi = 0$		for OI of $\psi = 0$	
	$m_1 = q_s \dfrac{\lambda_s}{n'_{s1}\lambda_1 - \lambda_s}$	$m_1 = q_s \dfrac{b_s}{n'_{s1}\varepsilon_{1s}b_1 - b_s}$	$n'_{s1} = 1$	$n'_{s1}\varepsilon_{1s} = 1$
	for the object image if $\psi_s = \psi_1 = \psi = 0$ and $n'_{s1} = 1$ (air medium)		for OI if $\psi = 0$ and $n'_{s1} = 1$	
	$m_1 = q_s \dfrac{\lambda_s}{\lambda_1 - \lambda_s}$	$m_1 = q_s \dfrac{b_s}{\varepsilon_{1s}b_1 - b_s}$	(−)	$\varepsilon_{1s} = 1$

Notes: 1. See Table 1, for explanation.

2. In [3], the phase jump differences ψ_1 and ψ_s on reflection were denoted, respectively, by $(\Delta\psi)_1$ and $(\Delta\psi)_2$. See also Notes to Table 1.

When compared with Eq. (2), the above relation means that the optical path difference δ produced by the object under study is a wavelength independent quantity, i.e., $\delta_s = \delta_1$.

The initial interference order m_1 can also be determined from the formula

$$m_1 = q_s \frac{b_s}{b_1 - b_s} \tag{6}$$

where b_1 and b_s are the interfringe spacings corresponding to the light wavelength λ_1 and λ_s. If this formula is ideally true for a given interferometric situation, we can also speak of the AVAWI method, but now interferometric adaptability functions in the domain of interfringe spacings. Adaptive interferometry of this kind will be denoted by AVAWI(b).

From Eq. (6) it follows that

$$(m_1 + q_s) b_s = m_1 b_1 . \tag{7}$$

When compared with formula (3), the above equation shows that the fringe displacement c produced by the object under study is a wavelength independent quantity if the AVAWI(b) method obeys. This also means that the zero-order interference fringe in the object image is ideally achromatic when white light is used.

In general, the AVAWI(b) method can occur more often in practice than the AVAWI(λ) method. However, the latter is usually the case of the reflected-light VAWI–1 technique [3] when an object under study and its substrate produce the same phase jumps on reflection without spectral dispersion and are surrounded by an air medium. In this instance the optical path difference δ is a wavelength independent quantity since it is simply equal to $2t$, where t is the object height. Except this situation, the AVAWI(b) method is generally more interesting and more suitable for many practical purposes.

A basic feature of the AVAWI(b) method is a kind of balancing of the spectral dispersions of refraction of the interferometric system and specimen under study (see the last columns of Tables 1 and 2). By contrast, the AVAWI(λ) method does not take advantage of the spectral dispersion of refraction of the interferometric system and requires the spectral dispersion of refraction of the examined object to be similar to that of a surrounding medium (see column 4 of Tables 1 and 2). This requirement is less practical than that on which the AVAWI(b) method is based. Consequently, we restrict our further discussion to the AVAWI(b) method used for the study of transparent objects.

3. Double-refracting AVAWI system

3.1. The VAWI–1 technique

Let the Biolar PI microinterferometer be used (see Fig. 7 in [1]). Its empty fringe interference field may be considered as a result of superposition of two wavefronts, laterally sheared and intersected with each other at a very small angle ε. This

angle is defined as

$$\varepsilon = 2(n_e - n_o)\tan\alpha = 2D\tan\alpha, \tag{8}$$

where $D = n_e - n_o$ is the birefringence of the crystal of which the main Wollaston prism of the microinterferometer is made, and α is the apex angle of this prism. The interfringe spacing b is given by $b = \lambda/\varepsilon$. Here λ is the wavelength of light used, which can be expressed as

$$\lambda = b\varepsilon = b2D\tan\alpha. \tag{9}$$

Consequently, the basic equations of the transmitted-light VAWI–1 technique [1], [2] may now be written as

$$\delta_1 = (n'_1 - n_1)t = m_1 b_1 2D_1 \tan\alpha \tag{10}$$

and

$$\delta_s = (n'_s - n_s)t = (m_1 + q_s)b_s 2D_s \tan\alpha \tag{11}$$

where n is the refractive index of the object under study, n' is that of a medium which surrounds the object, and t is the object thickness.

From Eqs. (10) and (11) it follows that

$$m_1 = q_s \frac{b_s}{N'_{s1} D_{1s} b_1 - b_s}, \tag{12}$$

where

$$N'_{s1} = \frac{n'_s - n_s}{n'_1 - n_1} = \frac{\delta_s}{\delta_1} = \frac{m_s \lambda_s}{m_1 \lambda_1} \tag{13}$$

and

$$D_{1s} = \frac{D_1}{D_s} = \frac{(n_e - n_o)_1}{(n_e - n_o)_s}. \tag{14}$$

Here the subscripts 1 and s refer to the wavelengths λ_1 and λ_s, respectively, for which the initial coincidence of interference fringes I and I' (Fig. **a**) and next a series of consecutive anticoincidences (Fig. **b**) and coincidences (Fig. **c**) of these fringes occur for $\lambda_s = \lambda_2 > \lambda_3 > \lambda_4 \ldots$. When compared with Table 1, the coefficient D_{1s} is equivalent to ε_{1s}.

The AVAWI(b) method holds good if the term

$$N'_{s1} D_{1s} = 1, \tag{15}$$

then Eq. (12) takes the form of Eq. (6)

In general, the coefficient D_{1s} is smaller than unity, while N'_{s1} may be either higher or smaller than unity. If, however, the object under study is surrounded by an air medium and its dispersion curve $n(\lambda)$ is normal, the coefficient N'_{s1} takes the

form

$$N'_{s1} = N_{s1} = \frac{1-n_s}{1-n_1} \tag{16}$$

and becomes higher than unity. It is therefore self-evident that condition (15) is more practical than $N'_{s1} = 1$ as the AVAWI(λ) method requires.

The first step in the AVAWI(b) procedure is to measure the interfringe spacings $b_s = b_1 > b_2 > b_3 \ldots$ corresponding to consecutive fringe coincidences (Fig. **a**, **c**) and anticoincidences (Fig. **b**) for particular wavelengths $\lambda_s = \lambda_1 > \lambda_2 > \lambda_3 \ldots$ and respective interference order increments $q_s = 0, 0.5, 1, \ldots$. The initial interference order m_1 is then calculated from Eq. (6), and the mean quantity

$$\overline{(m_1+q_s)b_s} = \overline{m_s b_s} = \frac{\sum_{s=1}^{S} (m_1+q_s)b_s}{S} = C \tag{17}$$

is determined. Here S is the total number of fringe coincidences and anticoincidences. If S is high, the anticoincident fringe configurations (Fig. **b**) may be ignored since they cannot visually be fixed so precisely as the coincident configurations (Figs. **a**, **c**). The fixation of these configurations is performed by sliding a wedge

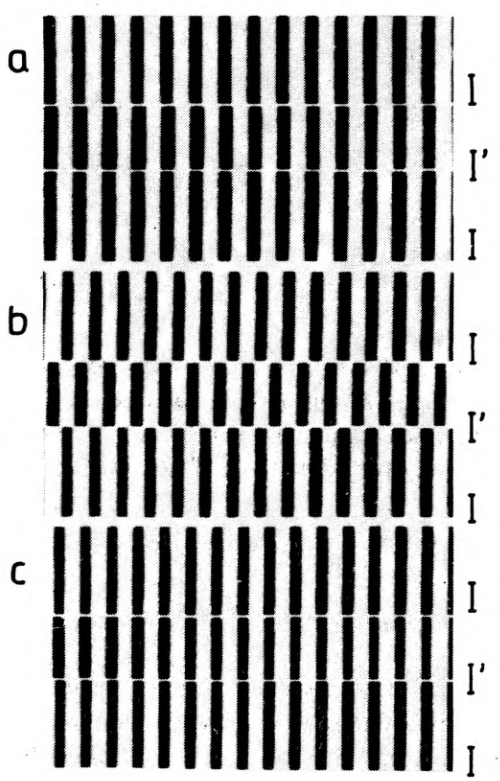

Coincident (**a** and **c**) and anticoincident (**b**) configurations of interference fringes observed in monochromatic light with decreasing wavelength. I – reference (undisplaced) fringes, I' – fringes displaced by a plate-like strip of a isotropic material. When the Biolar PI microinterferometer is used, the fringes I' correspond to one of two equivalent images sheared laterally (the objective birefringent prism is crossed with the main Wollaston prism)

interference filter which extracts monochromatic light of variable wavelength from a source of white light (halogen lamp). This filter especially well cooperates with the Biolar PI microinterferometer.

Formula (17) permits us also, if necessary, to "improve" these of the interfringe spacings b_s which have been measured for not ideally coincident and/or anticoincident configurations of interference fringes I and I' (Fig.). The improved interfringe spacings are given by $\bar{b}_s = C/(m_1 + q_s)$.

The particular wavelengths $\lambda_s = \lambda_1, \lambda_2, \lambda_3, \ldots$ corresponding to $b_s = b_1, b_2, b_3, \ldots$ can then be read out from the calibration plot $b(\lambda)$, and the optical path differences δ_s may be determined from the relations

$$\delta_s = (m_1 + q_s)\lambda_s = C\frac{\lambda_s}{b_s} \tag{18a}$$

or, in general,

$$\delta = C\frac{\lambda}{b}. \tag{18b}$$

The graph $\delta(\lambda)$, if necessary, can then be plotted. It may be useful, for instance, for determining the coefficients N'_{s1} or N_{s1} for other wavelengths than λ_1 and $\lambda_s = \lambda_2, \lambda_3, \lambda_4, \ldots$ (for λ_1 and λ_s the coefficients $N'_{s1} = \delta_s/\delta_1 = m_s\lambda_s/m_1\lambda_1$).

Equations (11) and (17) show that the optical path difference introduced by the object under study to the interference field can be expressed as

$$\delta_s = C2D_s \tan\alpha \tag{19a}$$

or more in general

$$\delta = C2D \tan\alpha \tag{19b}$$

where δ corresponds to a light wavelength λ for which the birefringence D of the main Wollaston prism * is exactly known. The Wollaston prisms of the Biolar PI microinterferometer are made of quartz crystal. The refractive indices n_o and n_e and the birefringence D of this crystal are very well known for many light wavelengths in both visible and invisible regions of the spectrum (see, e.g., [7]). We can therefore plot a graph $D(\lambda)$ from which one can read out D and calculate δ from Eqs. (19b) for arbitrary wavelengths λ. In this instance, the calibration graph $b(\lambda)$ is not necessary. In general, however, the graph $b(\lambda)$ is more advantageous since it is almost linear over the spectrum. Moreover, to use the graph $D(\lambda)$ and Eqs. (19), the apex angle α of the main Wollaston prism must exactly be known.

---

* The Biolar PI microinterferometer is standardly equipped with a double refracting system which uses simultaneously two double refracting prisms. One of them is located immediately behind the lens system of the microscope objectives PI, and the other, referred to as the main double refracting prism, is installed in the microscope tube arranged specially as an interferometric unit. However, the material and construction parameters of the objective birefringent prism are unimportant in the VAWI techniques and AVAWI approach.

As can readily be seen, Eqs. (11) and (17) and the relations (19) enable the thickness t of the object under study to be expressed as

$$t = \overline{(m_1 + q_s)\, b_s} \frac{2D_s}{n'_s - n_s} \tan\alpha = C \frac{2D_s}{n'_s - n_s} \tan\alpha \tag{20}$$

if the AVAWI(b) method holds good. Moreover, Eq. (15) yields $D_s/(n'_s - n_s) = D_1/(n'_1 - n_1)$. This relation means that the term $D_s/(n'_s - n_s)$ in Eq. (20) is a wavelength independent quantity and can therefore be taken as a parameter constant over the wavelength spectrum. If this parameter is known, the thickness t is determined more precisely than is usual since the only directly measured parameter that does enter the above equation is the interfringe spacing, which can be measured very accurately by using quite simple means.

On the other hand, if t and D_s are precisely known, the refractive index difference $n'_s - n_s$ can be expressed by

$$n'_s - n_s = C \frac{2D_s}{t} \tan\alpha \tag{21}$$

and thus determined more accurately than is usual.

Moreover, it is worthwhile noting that Eq. (17) permits us to determine additionally a number of interfringe spacings which cannot be measured. For instance, we are able to find several interfringe spacings (and respective light wavelengths from an extrapolated calibration plot $b(\lambda)$) in invisible regions of the spectrum when interference patterns and consecutive fringe coincidences and/or anticoincidences are only visually recorded. Consequently, we can determine optical path differences δ_s and related quantities, e.g., refractive indices n_s, within a larger spectral region than that which may directly be observed.

It will be interesting to analyse Eq. (15) and find the refractive indices n_C, n_e, and n_F of some hypothetical materials with different refractive index n_D, which apply to the AVAWI(b) method and to the Biolar PI microinterferometer fitted with the main Wollaston prism made of different birefringent crystals (quartz, calcite, ADP, KDP). For this analysis we can rewrite Eq. (15) in the form $N'_{sD} D_{Ds} = 1$ and assume $n'_D = 1$ and $n'_s = 1$ (air medium). As a result of this operation we have

$$n_s = 1 + \frac{D_s}{D_D}(n_D - 1). \tag{22}$$

Here the subscript s refers to the wavelengths $\lambda_F = 486.1$ nm, $\lambda_e = 546.1$ nm and $\lambda_C = 656.3$ nm, while the subscript D denotes the spectral line of wavelength $\lambda_D = 589.3$ nm. Some exemplary data obtained from the above equation are listed in Table 3, which shows that the materials in question belong to rather high-dispersion substances since their mean dispersion $n_1 - n_C$ is relatively high and the

Table 3. Optical data (refractive indices n, mean dispersion $n_F - n_C$, and Abbe number V_D) of some hypothetical materials which satisfy the requirements of the AVAWI(*b*) method applied to the double-refracting interferometer whose Wollaston prism is made of different birefringent crystals

Wollaston-prism material	n_D	n_C	n_e	n_F	$n_F - n_C$	$V_D = \frac{n_D - 1}{n_F - n_C}$
Quartz	1.40	1.3965	1.4029	1.4084	0.0119	33.6
$D_C = 0.009030$	1.45	1.4461	1.4533	1.4595	0.0134	33.6
$D_D = 0.009109$	1.50	1.4957	1.5037	1.5105	0.0148	33.6
$D_e = 0.009176$	1.55	1.5452	1.5540	1.5616	0.0164	33.6
$D_F = 0.009300$	1.60	1.5948	1.6044	1.6126	0.0178	33.6
$V_W = \frac{D_D}{D_F - D_C} = 33.6$	1.65	1.6444	1.6548	1.6637	0.0193	33.6
	1.70	1.6939	1.7051	1.7148	0.0209	33.6
Calcite	1.40	1.3950	1.4041	1.4119	0.0169	23.7
$D_C = 0.16983$	1.45	1.4444	1.4547	1.4634	0.0190	23.7
$D_D = 0.17197$	1.50	1.4938	1.5052	1.5149	0.0211	23.7
$D_e = 0.17376$	1.55	1.5432	1.5557	1.5664	0.0232	23.7
$D_F = 0.17709$	1.60	1.5925	1.6062	1.6179	0.0254	23.7
$V_W = \frac{D_D}{D_F - D_C} = 23.69$	1.65	1.6419	1.6568	1.6694	0.0275	23.7
	1.70	1.6913	1.7073	1.7208	0.0295	23.7
ADP	1.40	1.3912	1.4062	1.4132	0.0220	18.1
$D_C = 0.03775$	1.45	1.4401	1.4569	1.4649	0.0248	18.1
$D_D = 0.03867$	1.50	1.4889	1.5077	1.5166	0.0277	18.1
$D_e = 0.03933$	1.55	1.5379	1.5585	1.5682	0.0303	18.1
$D_F = 0.04025$	1.60	1.5868	1.6093	1.6199	0.0331	18.1
$V_W = \frac{D_D}{D_F - D_C} = 18.1$	1.65	1.6357	1.6600	1.6715	0.0358	18.1
	1.70	1.6845	1.7108	1.7232	0.0387	18.1
KDP	1.40	1.3905	1.4068	1.4163	0.0258	15.5
$D_C = 0.03775$	1.45	1.4393	1.4577	1.4684	0.0291	15.5
$D_D = 0.03867$	1.50	1.4881	1.5085	1.5204	0.0323	15.5
$D_e = 0.03933$	1.55	1.5369	1.5594	1.5725	0.0356	15.5
$D_F = 0.04025$	1.60	1.5857	1.6102	1.6245	0.0388	15.5
$V_W = \frac{D_D}{D_F - D_C} = 15.5$	1.65	1.6345	1.6611	1.6766	0.0421	15.5
	1.70	1.6833	1.7119	1.7286	0.0453	15.5

D_C, D_D, D_e, and D_F are the birefringences of crystals for spectral lines C, D, e, and F, respectively.

Abbe number

$$V = \frac{n_D - 1}{n_F - n_C} \tag{23}$$

is low.

Equation (22) may be rewritten as $n_F = 1 + D_F(n_D - 1)/D_D$ and $n_C = 1 + D_C(n_D - 1)/D_D$. When the right-hand sides of these equations are substituted into formula (23), we obtain

$$V = V_W = \frac{D_D}{D_F - D_C}, \tag{24}$$

where D_D, D_F, and D_C are the birefringence of the crystal of which the main Wollaston prism of the microinterferometer is made. Similarly, the mean dispersion $n_F - n_C$ of the materials in question is given by

$$n_F - n_C = \frac{(n_D - 1)}{V_W}. \tag{25}$$

Formulae (24) and (25) are accepted as practical conditions for the transparent materials which apply (or probably apply) to the double-refracting AVAWI(b) system discussed here.

3.2. The AVAWI–2 technique

The above presented basis of the AVAWI(b) approach is suitable for the study of objects which do not produce too small optical path differences δ, say, not smaller than 3λ. Otherwise, the number of fringe coincidences and/or anticoincidences (see Fig.) is small or even equal to zero within the visible spectrum, and the VAWI–1 technique becomes ineffective. This limitation is overcome by arranging interference fringe coincidences in another way (see [6], for details). For this operation a gauging graticule consisted of two pointer lines L_1 and L_2 (see Fig. 1 in [6]) is now employed. The distance d between these lines is selected as long as possible, say, $d = 10b_1$. One line L_1 is permanently brought into coincidence with the centre of the zero-order fringe I_0 of the empty interference field, while the consecutive high-order fringes are brought into coincidence with the other pointer line L_2 when the wavelength of monochromatic light is varied (decreased). Initially the empty interference field is processed (see Fig. 1 in [6]). Starting from long wavelengths permits us to select such a first clearly visible red wavelength λ_1 for which one of the high-order dark fringes becomes coincident with the pointer line L_2. Next, the light wavelength is continuously decreased from λ_1 to $\lambda_2, \lambda_3, \lambda_4, \ldots$, for which the pointer line L_2 becomes consecutively coincident with the bright, dark, bright, dark, etc., fringes whose interference orders are higher by $q_s = 0.5, 1, 1.5, 2, \ldots$ with respect to the initial interference order m_1 of the fringe which was initially coincident with the line L_2. For each of these coincident situations, the interfringe spacings $b_1, b_2, b_3, \ldots$ are measured and the initial interference order m_1 is determined.

As shown previously (see [6]), Eq. (6) applies strictly to the empty interference field, the basic condition of the AVAWI(b) is therefore fulfilled and we can take the mean quantity

$$\overline{(m_1 + q_s) b_s} = \overline{m_s b_s} = \frac{\sum_{s=1}^{S} (m_1 + q_s) b_s}{S} = E \tag{26}$$

where S is the total number of the fringe coincidences with the pointer line L_2.

The operation sketched above is then applied to the interference fringes displaced by an object under study (see Fig. 2 in [6]). The pointer line L_1 is, however, coincident with the centre of the zero-order fringe of the empty interference field as before. The AVAWI(b) approach now requires that Eq. (15) should be fulfilled (see Table 1) for transmitted light interferometry. If this holds good, we can take the mean quantity

$$\overline{(m_1+q_s)b_s} = \overline{m_s b_s} = \frac{\sum_{s=1}^{S}(m_1+q_s)b_s}{S} = C' \tag{27}$$

where m_1, m_s, b_s, and S are, of course, other than in Eq. (25), and only for small optical path differences δ the ininitial interference order m_1 and overal number of the coincidences of displaced interference fringes with the pointer line L_2 may be the same as for the empty interference field within the visible spectrum.

The optical path difference due to the object under study is determined from the formula

$$\delta = (C'-E)\frac{\lambda}{b} \tag{28}$$

for a given wavelength λ which corresponds with the interfringe spacing b read out from the calibration plot $b(\lambda)$. On the analogy of Eq. (19b), we can also write

$$\delta = (C'-E)\,2D\tan\alpha. \tag{29}$$

For this technique, Eqs. (20) and (21), in which only C should be replaced by $C'-E$, also obey.

The Biolar PI microinterferometer enables the object under study to be observed as two more or less laterally separated images. If the object is isotropic and uniform, the separated image portions are equivalent to each other, but one of them includes the positive value of δ and the other, the negative value of δ. The measurement procedure sketched above can be performed on both images or on their separated portions, and we obtain 2δ instead of δ as a result of measurement expressed by

$$2\delta = (C'-C'')\frac{\lambda}{b} \tag{30}$$

or

$$2\delta = (C'-C'')\,2D\tan\alpha. \tag{31}$$

Here C' and C'' are defined by Eq. (27), but C' refers to one of the separated image portions and C'', to the other. As can be seen, this situation does not require the empty interference field to be processed. Moreover, the measurement accuracy for δ is twice as good as that offered by Eqs. (28) and (29).

3.3. The VAWI-3 technique

There are sometimes interferometric situations which do not permit us to observe simultaneously the reference (undisplaced) interference fringes and the fringes displaced by the object under study. If, in this instance, the optical path difference δ to be measured is greater, say, than 5λ, neither the VAWI–1 technique nor the VAWI–2 procedure can effectively be used. This limitation is overcome by using the VAWI–3 technique [5], which is based on the same general principle as that of the VAWI–2 technique, but a single pointer line is used. Initially, the zero-order interference fringe of the empty field is brought into coincidence with this line, light wavelength is then varied (decreased), and high-order fringes displaced by the object under study are consecutively brought into coincidences with the pointer line, and respective interfringe spacings $b_1, b_2, b_3, \ldots$ are measured. The requirements of the AVAWI(b) method are the same as those described previously for the VAWI–1 technique (see Sect. 3.1 and Tab. 1). The optical path difference δ is determined from Eqs. (18) or (19).

4. The AVAWI (b) approach to birefringent objects

A double-refracting interferometer, like the Biolar PI microinterferometer, is especially suitable for measuring the birefringence B of double-refracting plates, birefringent fibres, and other anisotropic objects [5].

Let us consider a birefringent plate of thickness t, whose refractive indices for the fast and slow components of light wave are denoted, respectively, by n_α and n_γ. The plate is placed in the object plane of the Biolar PI microinterferometer and orientated diagonally with respect to the directions of light vibration in the crossed polarizer and analyser of the interferometer. The diagonal orientation means that the fast or slow axis of the examined plate forms an angle (azimuth) $\Theta = 45°$ or $-45°$ with the light vibrations in the crossed polars. Under these conditions, part of the image plane of the interferometer, where the sheared images of the plate overlap, contains information on the optical path difference δ due to the birefringence B of the plate under study. This optical path difference is expressed by

$$\delta = (n_\gamma - n_\alpha)\, t = Bt, \tag{32}$$

and is observed as an interference fringe displacement. On the analogy of Eqs. (10) and (11), we can write the following equations:

$$\delta_1 = B_1 t = m_1 b_1 2D_1 \tan\alpha, \tag{33a}$$

$$\delta_s = B_s t = (m_1 + q_s) b_s 2D_s \tan\alpha, \tag{33b}$$

from which it follows

$$m_1 = q_s \frac{b_s}{B_{s1} D_{1s} b_1 - b_s} \tag{34}$$

where $B_{s1} = B_s/B_1$. (It has tacitly been assumed that the birefringent plate is suitable for the VAWI–1 or VAWI–3 procedures). The above expression is identical with Eq. (12), but it contains the coefficient B_{s1} instead of N'_{s1}, which expresses the spectral dispersion of birefringence of the plate under study.

It is possible that the dispersion curves $B(\lambda)$ and $D(\lambda)$ satisfy the equation

$$B_{s1} D_{1s} = 1; \tag{35}$$

then the AVAWI(*b*) approach applies to this situation. Consequently, Eq. (34) takes the form of Eq. (6) or (7) and we have a new technique for very accurate interference metrology. First of all, the thickness t of birefringent plates can precisely be determined by measuring the only interfringe spacings. To show this possibility, let us write Eq. (33b) in the form

$$t = \overline{(m_1 + q_s) b_s} \frac{D_s}{B_s} 2\tan\alpha = C \frac{D_s}{B_s} 2\tan\alpha. \tag{36}$$

If Eq. (35) holds good, the term D_s/B_s is constant and wavelength independent quantity. In particular, B_s may be equal to D_s and the above equation reduces simply to

$$t = C2\tan\alpha \tag{37}$$

where C is defined by Eq. (17) and α is the apex angle of the main Wollaston prism of the Biolar PI microinterferometer. The angle α is a quantity valid in perpetuity and can be determined extremely accurately. There is no problem in securing $\Delta b = \pm 0.01$ μm for b_s. This enables the thickness t to be measured with an accuracy equal to or even better than $\Delta t = \pm 0.0001t$ if δ is not smaller than several, say, 5 μm.

If, however, the optical path difference δ is small, say, smaller than 3λ, the AVAWI(*b*)–2 procedure can be applied. This procedure also requires the condition (35) to be fulfilled. A birefringent plate to be measured may be orientated at $\Theta_L = +45°$ (left-hand diagonal position) and next at $\Theta_R = -45°$ (right-hand diagonal position), and the processing of the empty interference field can be ignored. In this instance, the plate thickness t is given by

$$t = |C_L - C_R| \frac{D_s}{B_s} 2\tan\alpha \tag{38}$$

or

$$t = |C_L - C_R| 2\tan\alpha \tag{39}$$

if $B_s = D_s$. Here C_L and C_R refer, respectively, to Θ_L and Θ_R and are defined by Eq. (26).

5. An illustrative example

Practical performance of the AVAWI(*b*) method is illustrated by Table 4, where the results of an exemplary experiment performed on a birefringent quartz plate are listed. The plate was cut parallely to the optic axis of quartz crystal. The Biolar PI microinterferometer and its $10\times$ PI objective were used. The objective double refracting prism was orientated subtractively with respect to the main quartz Wollaston prism No. 2. The requirements of the AVAWI(*b*) were ideally fulfilled. Since the plate produced $\delta_1 = 10\lambda_1$, the VAWI–3 technique was used and the thickness t was determined from Eq. (37). The apex angle α of the main Wollaston prism mentioned above was equal to 9°3′53″. The thickness t of the examined quartz plate was determined to be equal to 653.30 μm. Then the birefringence $B = n_\gamma - n_\alpha = n_e - n_o$ of the quartz crystal was determined for a series of light wavelengths from both the visible and invisible (near UV and IR) regions of the spectrum. The results are listed in the last column of Table 4. In the author's opinion, these results are much more accurate than those given in different literature sources and are comparable, with a discrepancy not higher than ± 0.000002, to the data which can be found in [7].

Table 4. Results of the measurement of a quartz birefringent plate by using the AVAWI(*b*)–3 technique and double-refracting microinterferometer Biolar PI

q_s	$m_s = m_1 + q_s$	b_s [μm]	$m_s b_s$ [μm]	$\overline{b_s} = \overline{m_s b_s}/m_s$ [μm]	λ_s [nm]	$\delta_s = m_s \lambda_s$ [μm]	$B = n_e - n_o = \delta_s/t$
−3	7	–	–	292.49	829.0	5.8030	0.008889
−2.5	7.5	–	–	273.00	777.5	5.8313	0.008926
−2	8	–	–	255.93	732.2	5.8576	0.008966
−1.5	8.5	–	–	240.87	691.5	5.8778	0.008998
−1	9	–	–	227.49	655.7	5.9013	0.009033
−0.5	9.5	215.45	2046.775	215.52	623.4	5.9222	0.009065
0	10 (= m_1)	204.65	2046.500	204.74	594.6	5.9460	0.009101
0.5	10.5	194.94	2046.870	194.99	568.6	5.9703	0.009139
1	11	186.01	2046.110	186.13	545.1	5.9961	0.009178
1.5	11.5	178.20	2049.300	178.04	523.8	6.0237	0.009220
2	12	170.84	2050.080	170.62	504.0	6.0480	0.009258
2.5	12.5	163.85	2048.125	163.79	486.0	6.0750	0.009300
3	13	157.36	2045.680	157.49	469.4	6.1022	0.009341
3.5	13.5	151.65	2047.275	151.66	454.1	6.1304	0.009383
4	14	146.25	2047.500	146.24	439.7	6.1558	0.009423
4.5	14.5	–	–	141.20	426.6	6.1857	0.009468
5	15	–	–	136.49	414.3	6.2145	0.009512
5.5	15.5	–	–	132.09	403.0	6.2465	0.009561
6	16	–	–	127.96	392.3	6.2768	0.009608
6.5	16.5	–	–	124.09	382.5	6.3113	0.009661
7	17	–	–	120.44	373.1	6.3427	0.009709

$\overline{m_s b_s} = 2047.4215$ μm, plate thickness $t = m_s b_s 2\tan\alpha = 653.30$ μm

Some other interesting experiments which illustrate the high performance of the AVAWI(*b*) method have been carried out (e.g., on polymeric textile fibres) and the results will be presented in separate papers.

6. Conclusions

Object-adapted variable wavelength interferometry presented in this paper cannot be considered as a universal method; it offers us rather a special, but simple and accurate tool for the study of some selected objects whose optical properties satisfy the requirements of this method.

Especially double-refracting interferometric systems which use Wollaston prisms are suitable for this kind of interferometry. The Wollaston prisms can be made of different birefringent crystals, whose spectral dispersion of birefringence appears to be similar to or even indentical with the spectral dispersion of the refractive index and/or of the birefringence of transparent objects and materials to be examined or tested in transmitted light.

In comparison to the common interferometric techniques, which use monochromatic light of constant wavelength, the AVAWI(*b*) method is more accurate (by one or even two orders of magnitude) and free from difficulties or even possible errors in establishing the integral number of interfringe spacings by which the object under study displaces interference fringes. If the requirements of the AVAWI(*b*) method are fulfilled, the zero-order fringe is achromatic in white light among the displaced interference fringes. However, the reverse is not always right. Frequently we can observe an ideally achromatic fringe in white light, but its order differs from zero and can lead to incorrect identification of interference fringes and thus to serious errors. The VAWI techniques permit us to overcome this limitation and, moreover, if the requirements of the AVAWI(*b*) method are confirmed (by the same or nearly the same products $m_s b_s$ within the visible spectrum), then the AVAWI(*b*) procedure can be applied and give more accurate interferometric results than any other technique.

Furthermore, if the AVAWI(*b*) method applies to a given object within a spectral region larger than the visible spectrum, then quantitative information on optical properties (refraction, birefringence) of the object can simply be derived from the results of measurement obtained only in a portion of the visible spectrum (see Table 4 and its upper and bottom parts).

Acknowledgments – I wish to thank Dr K. Pietraszkiewicz and Dr W. Urbańczyk from the Institute of Physics, Technical University of Wrocław, for a constructive discussion of Table 4 and for indication Ref. [7], where detailed data concerning the refractive indices (n_o, n_e) of quartz crystal are given for a large spectral region (from 300 to 2000 nm).

References

[1] PLUTA M., Opt. Appl. **15** (1985), 375–393.
[2] PLUTA M., Opt. Appl. **16** (1986), 141–157.

[3] PLUTA M., Opt. Appl. **16** (1986), 159–174.
[4] PLUTA M., Opt. Appl. **16** (1986), 301–323.
[5] PLUTA M., Opt. Appl. **17** (1987).
[6] PLUTA M., Opt. Appl. **17** (1987).
[7] ZOLOTARIEV V. M., MOROZOVA V. N., SMIRNOVA E. V., *Opticheskie postoyannye prirodnikh i tekhnicheskikh sred, Spravochnik* (in Russian), Khimiya, Leningrad 1984, p. 105.

Received August 7, 1987

Интерферометрия с непрерывно переменной длиной световой волны. VII. Метод адаптированный к объекту

Описанные раньше меторы интерферометрии с непрерывно переменной длиной световой волны заключают в себе два специфических варианта, которые можно назвать адаптированной интерферометрией. Один из этих вариантов действует в диапазоне длины волны, другой в диапазоне интерференционного периода. Второй вариант является более надобным для интерферометрии в проходящем свете, первый же для интерферометрии в отраженном свете предметов находящихся в воздушной среде.